XXXVI Ibero-Latin American
Congress on Computational
Methods in Engineering
CILAMCE
Rio de Janeiro, 22-25 Nov
2015

3D OcTree Finite-volume method for acoustic wave simulation

André Valente

andre.valente@ifrj.edu.br

Instituto Federal de Educação, Ciência e Tecnologia do Rio de Janeiro, Av. República do Paraguai, 120, 25050-100, Duque de Caxias-RJ, Brasil.

Leandro Di Bartolo

dibartolo@on.br

Observatório Nacional / MCTI – Departamento de Geofísica (COGE), R. General José Cristino, 77, São Cristóvão, 20921-400, Rio de Janeiro-RJ, Brasil.

Webe João Mansur

webe@coc.ufrj.br

Universidade Federal do Rio de Janeiro / COPPE / LAMEMO, Av. Pedro Calmon s/no. – Prédio Anexo ao Centro de Tecnologia – Ilha do Fundão, 21941-596, Rio de Janeiro-RJ, Brasil.

Abstract. *Because the grid spacing is fixed in the finite-difference method (FDM), the numerical dispersion usually imposes the use of restrictive small grid spacing in the whole model. In consequence, the number of grid points per wave-length usually is too large in deep layers for seismic modeling applications, resulting in loss of efficiency of the FDM. Although the use of high-order operators allows bigger grid spacing and, in principle, could make FDM more efficient, this does not solve the problem. We develop a new 3D explicit scheme based on finite-volume method (FVM) that addresses the aforementioned problem using OcTree meshes. In this paper, we present the construction of the method and the first modeling results carried out in a simple but realistic model. The 3D algorithm is constructed using a general formalism with sparse matrices and it allows both the use of different grid spacing in layers with different velocities and the refinement in regions of interest. The OcTree mesh is easy to generate using simple criterion from a regular grid, avoiding additional complications in meshing. Computational tools for parallel processing on the GPU were used for the algebraic manipulation of the sparse matrices. The numerical scheme can be seen as an extension of the staggered-grid scheme: it reduces to the classical staggered-grid scheme for the case of regular grids.*

Keywords: *3D Wave Propagation, OcTree Meshes, Seismic waves, acoustics*

1 INTRODUCTION

Wave propagation problems often appear in various areas of science, especially in engineering and applied geophysics. In regions where the propagation medium is complex, the use of efficient numerical methods to obtain approximate solutions to hyperbolic wave equations plays a central role in several important applications. In geophysics, examples can be found in imaging of subsurface structures and in inversion.

This paper focuses on geophysics applied to petroleum. The huge challenges in exploration and reservoir characterization put the wave equation based algorithms in highlight, making full waveform inversion (FWI), used to obtain the velocity model for example, and reverse time migration (RTM), a powerful method for imaging subsurface structures, important tools in the industry. Offshore salt tectonics regions became common exploration targets in oil industry and, at present, it is well known that a significant proportion of the world hydrocarbon reserves are in structures related to these geological formations. In many places around the world, great interest has been focused in pre-salt geologic formations. These areas are hard to illuminate and very complex geologically, being present layers with high-velocity together with lower velocities, all below thousands of meters of the water surface. On the other hand, the technological development in acquisition and processing has allowed images with increasing resolution and incredible final quality.

In this context, developing powerful and efficient numerical schemes for seismic modeling has fundamental importance. The finite-difference method (FDM) is the most popular method used to model seismic waves, mainly because of its simplicity and robustness. FDM is one of the most simple methods to implement and it is very suitable to parallelization. It is applicable in a simple way to complex regions and it is relatively accurate and computationally efficient. However, the FDM is not free of inherent limitations: some of the main limitations are the difficult to handle accurately irregular interfaces between discontinuous material layers and the fixed and too small grid spacing imposed by numerical dispersion (specially in high-velocity layers), in addition to impossibility of local refinement.

In FDM-based algorithms, the price to use a regularly spaced grid is that a restrictive small grid spacing must be used in the whole model, imposed by the lower velocity present in the geophysical medium. This makes the number G of grid points per wave-length too large in high-velocity layers, making these schemes lose efficiency. Although the use of high-order operators allows bigger grid spacing and, in principle, it could make FDM more efficient, this does not solve the problem and yet worsens another problem: specially in applications using high-resolution data, it causes possible loss of resolution because of the pixel size too big in relation to the nominal resolution.

The introduction of staggered grids schemes (hereafter, SSG) using FDM by Virieux (1986) is considered a major step in seismic modeling (Moczo et al., 2002), being the SSG schemes (Levander, 1988; Graves, 1996) the most applied algorithms for seismic modeling and applications. One of the better advantages of these schemes is its low sensitivity on Poison's ratio in elastic wave propagation and the superior accuracy compared with single-grid FDM schemes. However, SSG does not solve the aforementioned limitations. Di Bartolo et al. (2011) proposed the equivalent staggered-grid (ESG) scheme, a FDM scheme numerically equivalent to the SSG scheme for acoustics, in terms of only the pressure field. Extensions to elastic wave equation were recently presented in Di Bartolo et al. (2015). The ESG schemes require less computational memory than SSG, although it remains with the limitations of the FDM mentioned previously.

In this paper, we develop a new 3D explicit scheme based on finite-volume method (FVM) that addresses the aforementioned problems, aiming to remain with relatively simple meshing yet. Here, we discuss its application to the simplest case, in acoustics. The algorithm allows local refinement using OcTree meshes, a good compromise between structured and unstructured meshes that makes meshing as easy as possible. In this sense, the OcTree can be generated directly from a regular grid using simple criteria. Hence, it is possible to make local refinement, e.g., in any interface, salt flanks and/or target layers, in a simple way. Also, the refinement can be adopted at the surface of onshore regions, specially in the presence of topography, using a vacuum condition, in order to guarantee a sufficient number of points per wavelength to guarantee the modeling accuracy (Robertsson, 1996).

The method proposed here is based on the method proposed by Horesh and Haber (2011) to solve Maxwell equations in quasi-static regime. Actually, it can be seen as an extension of the SSG scheme for OcTree meshes: it reduces to the SSG scheme for the case of regular grids or, specifically, to the ESG scheme in terms of only the pressure (Di Bartolo et al., 2011). The algorithm is constructed using a general formalism with sparse matrices and allows both the use of different grid spacing in layers with different velocities and the refinement in regions of interest. Computational tools for parallel processing on the GPU were used for the manipulation of the sparse matrices (Bell and Garland, 2012). The paper is structured as follows. In the next section, we present the acoustic wave equation used. Section 3 shows the details about the numerical formulation developed. The Section 4 presents a numerical example to show the effectivity of the developed method. Finally, the conclusions are addressed.

2 ACOUSTIC WAVE EQUATION

The description of acoustic wave propagation, in terms of velocity and pressure, is obtained using Newton second law and continuity equation with adiabatic assumption at the equation of state. The following coupled first-order system is obtained (Wapenaar and Berkhout, 1989)

$$\rho(\vec{r})\frac{\partial \vec{v}(\vec{r},t)}{\partial t} + \vec{\nabla} p(\vec{r},t) = \vec{f}(\vec{r},t) \tag{1}$$

$$\frac{1}{\kappa(\vec{r})}\frac{\partial p(\vec{r},t)}{\partial t} + \vec{\nabla}.\vec{v}(\vec{r},t) = \frac{\partial i_V(\vec{r},t)}{\partial t}, \tag{2}$$

where $\vec{v}$ is the velocity vector, p is the acoustic pressure, $\vec{r}$ is the position vector, t is the time, ρ is the density of the medium, $\vec{f}$ is the density of external body force applied, $\partial/\partial t$ is the time derivative and $\vec{\nabla} = (\partial/\partial x, \partial/\partial y, \partial/\partial z)$ in Cartesian coordinates, κ is the adiabatic compression modulus of the medium and i_V, which represents a source, is a volume density of volume injection (an air gun, for example). By eliminating the velocity field from the set of Eqs 1-2, the acoustic wave equation in terms of pressure only can be obtained as

$$\rho\vec{\nabla}.\left(\frac{1}{\rho}\vec{\nabla}p\right) - \frac{1}{c^2}\frac{\partial^2 p}{\partial t^2} = -s, \tag{3}$$

where s and c are, respectively, the source and wave velocity:

$$s = \rho\frac{\partial^2 i_V}{\partial t^2} - \rho\vec{\nabla}.\left(\frac{1}{\rho}\vec{f}\right), \quad c = \sqrt{\frac{\kappa}{\rho}}. \tag{4}$$

3 NUMERICAL FORMULATION

This section presents the details about the FVM-based numerical formulation implemented, applied to the acoustic wave propagation. The matrix formalism is close to the presented by Horesh and Haber (2011). First we present the OcTree mesh generation, then we develop the numerical operators using FVM. A simple example for the operators in a 2D small mesh is presented. Afterwards, the non-reflecting boundary conditions used are described and the final time marching equation is presented.

3.1 OcTree Mesh Generation

An OcTree mesh (see Fig. 1) can be represented by a sparse three-dimensional matrix

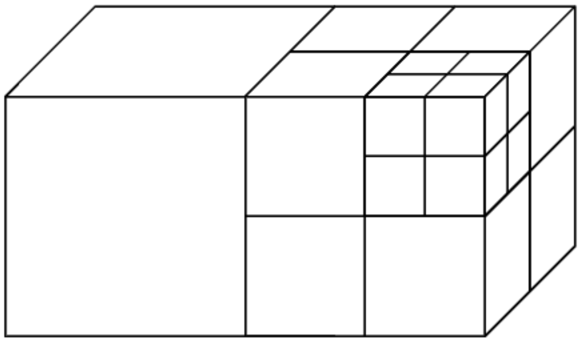

Figure 1: A small OcTree Mesh.

$M_{i,j,k}$, with dimensions $n_x \times n_y \times n_z = 2^a \times 2^b \times 2^c$, where its non-zero values are also powers of 2. Let h be the grid spacing corresponding to one unit of the mesh, hence the total dimensions of the mesh are given by the dimensions of M multiplied by h. Then, the non-zero values of the mesh represent cubic volumes with edges given by the product of these values by h. In this paper, it is required that the OcTree mesh is balanced, i.e., the ratio between neighbors volumes edges must be 1/2, 1 or 2. Figure 1 shows an example of mesh with dimensions $2^3 \times 2^2 \times 2^2$, where the M matrix is given by

$$M_{*,*,1} = \begin{pmatrix} 4\,0\,0\,0\,2\,0\,2\,0 \\ 0\,0\,0\,0\,0\,0\,0\,0 \\ 0\,0\,0\,0\,2\,0\,1\,1 \\ 0\,0\,0\,0\,0\,0\,1\,1 \end{pmatrix} M_{*,*,2} = \begin{pmatrix} 0\,0\,0\,0\,0\,0\,0\,0 \\ 0\,0\,0\,0\,0\,0\,0\,0 \\ 0\,0\,0\,0\,0\,0\,1\,1 \\ 0\,0\,0\,0\,0\,0\,1\,1 \end{pmatrix} M_{*,*,3} = \begin{pmatrix} 0\,0\,0\,0\,2\,0\,2\,0 \\ 0\,0\,0\,0\,0\,0\,0\,0 \\ 0\,0\,0\,0\,2\,0\,2\,0 \\ 0\,0\,0\,0\,0\,0\,0\,0 \end{pmatrix} M_{*,*,4} = \begin{pmatrix} 0\,0\,0\,0\,0\,0\,0\,0 \\ 0\,0\,0\,0\,0\,0\,0\,0 \\ 0\,0\,0\,0\,0\,0\,0\,0 \\ 0\,0\,0\,0\,0\,0\,0\,0 \end{pmatrix}.$$

Concerning the OcTree mesh generation, a criterion that considers both the propagation velocity and the proximity with interfaces and/or target thin regions can be used. Due to practical purpose, it is considered first a fine regular mesh (a grid) that will be used as input to generate the OcTree mesh. We apply an specific criterion on the input grid to set the dimensions of OcTree volumes and generate M, according with the velocity and according whether the volume is close to an interface. In the volumes near the interface for example, the mesh is kept with the smaller size (the original size of the input grid) and it is progressively coarsened up to the target size of the volume chosen for the layer both for the layer below and for the layer above this interface. The best criterion to choose the target size of the volumes is: the bigger possible dimension to avoid numerical dispersion, corresponding to an ideal G (points per wave-length).

3.2 Discretization of differential operators

The usual FVM flux-balance approach (Dormy and Tarantola, 1995) is used to construct the operators. First, we deal with the divergent operator. Using Gauss theorem, we can write

$$\int_V \vec{\nabla} \cdot \vec{J} dV = \int_S \vec{J} \cdot \hat{n} dS, \tag{5}$$

where V is the volume, S is its surface, $\vec{J}$ is a flux density vector vector field and $\hat{n}$ is the unitary vector pointing outward S. We can approximate the divergent (at a polyhedral volume v_i) as

$$\vec{\nabla}.\vec{J_i} \approx \frac{1}{\mathrm{Vol}(v_i)} \sum_{j=1}^{n} \int_{f_j} \vec{J} \cdot \hat{n} dS, \tag{6}$$

where f_j are the faces delimiting v_i and $\mathrm{Vol}(v_i)$ is v_i volume.

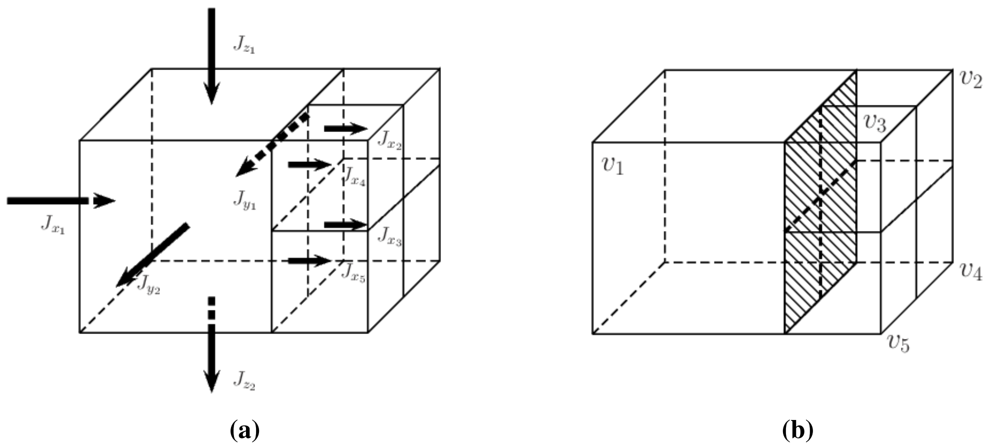

Figure 2: Approximation for (a) the divergent and (b) the gradient operators.

The fact that the volumes of OcTree mesh are cubes allows easy calculation. For example, considering the Fig. 2a, the finite volume approximation at v_j (at left side) for divergent is

$$\vec{\nabla}.\vec{J_i} \approx \frac{1}{2^{3n}h^3} \left[2^{2n}h^2(J_{x_1} + J_{y_1} - J_{y_2} + J_{z_1} - J_{z_2}) - 2^{2(n-1)}h^2(J_{x_2} + J_{x_3} + J_{x_4} + J_{x_5}) \right],$$

where $h_i = h2^n$ is the edge size of the volume v_i.

To construct the numerical scheme in a general way (using an M matrix), it is necessary to numbering all the n_v volumes and all the n_f faces. Then, we construct a diagonal matrix V, with dimensions $n_v \times n_v$, where the elements are the volumes of v_i; and a diagonal matrix F, with dimensions $n_f \times n_f$, where the elements are the edge dimensions of the faces f_i.

Another important matrix is the sparse matrix N (dimensions $n_v \times n_f$), that connects the volumes with their faces. Its elements are defined as $N_{i,j} = \pm 1$ if f_j belongs to v_i. If $\vec{J}$ (see Fig. 2a) is directed to the inside (outside) of the v_i, $N_{i,j} = +1$ ($N_{i,j} = -1$)

Using these matrices, the divergent operator can be written as matrix product given by

$$\mathrm{Div} = \frac{1}{h} V^{-1} N F^2. \tag{7}$$

Lets consider the gradient operator. For example, considering the face f_i shown in Fig. 2b, the finite volume approximations for the component x of gradient at f_i is:

$$\left(\vec{\nabla} P\right)_i \backsimeq \frac{P_2 + P_3 + P_4 + P_5}{h2^{(n-1)}} - \frac{P_1}{h2^n}, \tag{8}$$

where P_i is the discrete pressure field considered at v_i.

Using the matrices defined previously, the gradient operator is

$$\mathrm{Grad} = -\frac{1}{h} F^{-1} N^T. \tag{9}$$

3.3 Simple Example

To illustrate the construction of the matrices, it will be used a small mesh in two dimensions with only three volumes and ten faces, as depicted in Fig. 3. Let the smaller squares have side

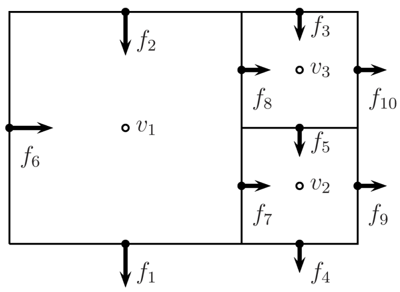

Figure 3: Small 2D mesh example.

2^n and the largest 2^{n+1}. The matrix M for the mesh presented in Fig. 3 can be easily obtained and the derived matrices are given by

$$V = \begin{pmatrix} 2^{n+1} & 0 & 0 \\ 0 & 2^n & 0 \\ 0 & 0 & 2^n \end{pmatrix} F = \begin{pmatrix} 2^{n+1} & 0 & 0 & 0 & 0 & 0 & 0 & 0 & 0 & 0 \\ 0 & 2^{n+1} & 0 & 0 & 0 & 0 & 0 & 0 & 0 & 0 \\ 0 & 0 & 2^n & 0 & 0 & 0 & 0 & 0 & 0 & 0 \\ 0 & 0 & 0 & 2^n & 0 & 0 & 0 & 0 & 0 & 0 \\ 0 & 0 & 0 & 0 & 2^n & 0 & 0 & 0 & 0 & 0 \\ 0 & 0 & 0 & 0 & 0 & 2^{n+1} & 0 & 0 & 0 & 0 \\ 0 & 0 & 0 & 0 & 0 & 0 & 2^n & 0 & 0 & 0 \\ 0 & 0 & 0 & 0 & 0 & 0 & 0 & 2^n & 0 & 0 \\ 0 & 0 & 0 & 0 & 0 & 0 & 0 & 0 & 2^n & 0 \\ 0 & 0 & 0 & 0 & 0 & 0 & 0 & 0 & 0 & 2^n \end{pmatrix} N^T = \begin{pmatrix} -1 & 0 & 0 \\ 1 & 0 & 0 \\ 0 & 0 & 1 \\ 0 & -1 & 0 \\ 0 & 1 & -1 \\ 1 & 0 & 0 \\ -1 & 1 & 0 \\ -1 & 0 & 1 \\ 0 & -1 & 0 \\ 0 & 0 & -1 \end{pmatrix}.$$

Then, the divergent operator can be obtained by means of the correct matrix products, as defined by Eq. 7, and is given by

$$\mathrm{Div} = \begin{pmatrix} -\frac{2^{2(n+1)}}{h2^{n+1}} & \frac{2^{2(n+1)}}{h2^{n+1}} & 0 & 0 & 0 & \frac{2^{2(n+1)}}{h2^{n+1}} & -\frac{2^{2n}}{h2^{n+1}} & -\frac{2^{2n}}{h2^{n+1}} & 0 & 0 \\ 0 & 0 & 0 & -\frac{2^{2n}}{h2^{n}} & \frac{2^{2n}}{h2^{n}} & 0 & \frac{2^{2n}}{h2^{n}} & 0 & -\frac{2^{2n}}{h2^{n}} & 0 \\ 0 & 0 & \frac{2^{2n}}{h2^{n}} & 0 & -\frac{2^{2n}}{h2^{n}} & 0 & 0 & \frac{2^{2n}}{h2^{n}} & 0 & -\frac{2^{2n}}{h2^{n}} \end{pmatrix}.$$

It should be noted that the line i of Div array contains the information of the faces that have influence on v_i. According to the construction and the notation used, v_i does not necessarily have six faces. For example, the volume at left presented in Fig. 2a has nine faces, with five sides with edges $h2^{n+1}$ and four sides with edges $h2^n$. It is worth nothing that the diagonal matrix F determines the size of each face. Another point to be stressed is that the divergent operator uses information contained in the faces and volumes, similar to staggered-grid FDM operators.

The gradient operator, defined by Eq. 9, can be calculated as

$$\mathrm{Grad}^T = \begin{pmatrix} \frac{1}{h2^{n+1}} & -\frac{1}{h2^{n+1}} & 0 & 0 & 0 & -\frac{1}{h2^{n+1}} & \frac{1}{h2^{n}} & \frac{1}{h2^{n}} & 0 & 0 \\ 0 & 0 & 0 & \frac{1}{h2^{n}} & -\frac{1}{h2^{n}} & 0 & -\frac{1}{h2^{n}} & 0 & \frac{1}{h2^{n}} & 0 \\ 0 & 0 & -\frac{1}{h2^{n}} & 0 & \frac{1}{h2^{n}} & 0 & 0 & -\frac{1}{h2^{n}} & 0 & \frac{1}{h2^{n}} \end{pmatrix}.$$

3.4 Boundary Conditions

Non-reflective boundary conditions proposed by Reynolds (1978) were applied, i.e., we considered one-way wave equation at the boundary volumes. For the application of this boundary condition in the proposed explicit scheme it is necessary to know, for each volume v_i, its neighbor in the direction normal to the boundary (named as v_i^{N}). Which results explicitly in

$$p^{n+1}(v_i) = p^n(v_i) - \frac{c\Delta t}{h}\left[p^n(v_i) - p^n(v_i^{\mathrm{N}})\right]. \tag{10}$$

However, this approach alone is not sufficient for satisfactory attenuation of reflection from the boundaries. It was necessary then another complementary approach. The absorbing layers method proposed by Cerjan et al. (1985) was adapted to our method and it was applied too.

3.5 Final Formulation

Using operators described previously, the discretization of the Eq. 3 is easily carried out. Let P_i be the discrete pressure field in a volume v_i of the OcTree Mesh M. We define new diagonal matrices: the B matrix, with dimensions $n_v \times n_v$, where $B_{i,i} = \Delta t^2 c_i^2 \rho_i / h^2$ for each v_i, the L matrix, with dimensions $n_f \times n_f$, where $L_{i,i}$ is the harmonic mean of the density of neighboring volumes that have f_i as face. Lastly, we define S, a very sparse $n_v \times n_v$ matrix, such that its only non-zero value $S_{i,i}$ is the value of the seismic source s when it is located in v_i. Finally, using the discrete operators, we can write the final explicit formulation as

$$P^{n+1} = YP^n + 2P^n - P^{n-1} + S^n, \tag{11}$$

where $Y = BV^{-1}NF^2LF^{-1}N^T$.

4 NUMERICAL EXAMPLE

To implement the numerical scheme, we have used the C language in Ubuntu Linux system running in an 4X AMD Opteron 6376 Abu Dhabi 2.3GHz with 258 GiB. Computational tools were used for processing on the GPU (NVIDIA Tesla C2075), the CUSP library (Bell and Garland, 2012), where the algebraic manipulation of a sparse matrix is made very efficiently.

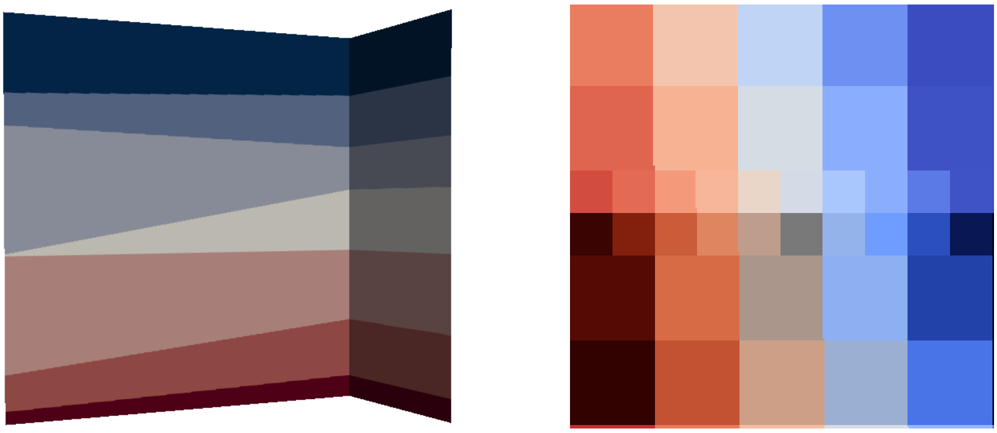

(a) (b)

Figure 4: (a) Syntetic Model with pinchout and salt layer and (b) Mesh Refinement at reflector.

As depicted in Fig. 4a, a small regular input synthetic model of seven inclined layers is used. The total number of points is $(n_x, n_y, n_z) = (2^9, 2^9, 2^9)$ and the grid spacing adopted is $h = 1.3m$ (the lowest h of the OcTree mesh) and hence the model is a cube with $665.6m$ of edge. The layer velocities are $c_1 = 1.5km/s$, $c_2 = 2.0km/s$, $c_3 = 2.5km/s$, $c_4 = 3.0km/s$, $c_5 = 4.5km/s$, $c_6 = 3.5km/s$ and $c_7 = 3.8km/s$; and the density is $\rho = 1,000kg/m^3$ in the whole model. The OcTree mesh generated in this example is very simple: the volumes near the interfaces are refined (edge size h) and the volumes at the layers has edge $2h$, as shown in Fig. 4b. In this example, we have $n_v = 18,461,698$ and $n_f = 56,378,628$. The time step adopter was $\Delta t = 0.32\,ms$ and a Ricker pulse source was used (placed at $z = 20.8m$) with frequency $f_{\text{cutoff}} = 80Hz$. The receivers are located at depth $z = 10.4m$.

Figure 5a shows the 2D synthetic seismogram obtained and Fig. 5b shows orthogonal slices of the 3D snapshots at time $t = 0.336s$. Figure 6 shows four snapshot slices. It can be seen clearly that the acoustic wave propagates well in the medium, without artifacts and without dispersion. The boundary reflections were very attenuated. In the next steps of the research, we will implement Perfect Matched Layers (Berenger, 1994). The effectiveness of the boundary conditions implemented can be seen in the seismogram (Fig. 5a). It shows all the reflections hyperbole from interfaces but the reflections from boundary is absent. It is worth noting that

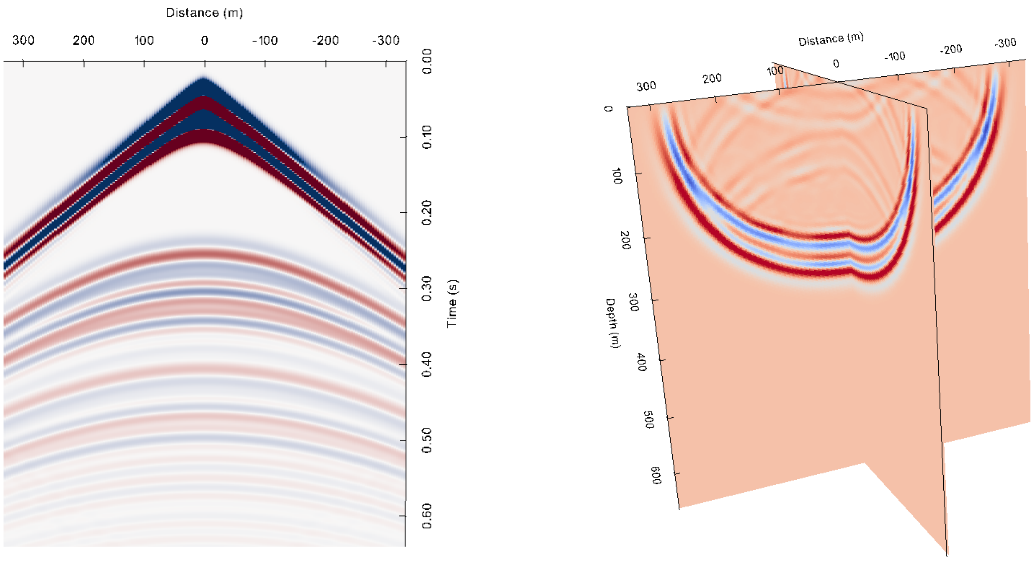

(a) **(b)**

Figure 5: (a) Synthetic seismogram and (b) 3D slices snapshot at $t = 0.336s$

the volume sizes of $2.6m$, in the first layer, means that the number of points per wave-length is $G = 7.2$. In refined region of this layer, $G = 14.4$. In the other layers, $G > 9.5$.

5 CONCLUSIONS

We have developed a 3D explicit time-marching finite-volume algorithm. The method was applied to acoustic wave propagation. The obtained numerical scheme is a generalization of the standard staggered-grid scheme (for acoustics) to allow local refinement using OcTree meshes. Actually, it is a generalization of the 3D ESG scheme presented by Di Bartolo et al. (2012). The OcTree mesh can be generated easily from a previous refined FDM grid using simple criteria, avoiding the complications raised with unstructured meshing. Beyond to avoid complications in meshing, the OcTree mesh gives rise to formulations with very good condition numbers because it does not suffer from geometry problems as can occurs in meshing with more complex elements. The resulting method is robust and efficient and it seems to work well according to the numerical example presented. The scheme is very promising for seismic modeling, as well as its applications in migration and inversion (e.g., RTM and FWI). The possibility of using different volume sizes can be responsible both by the better efficiency and resolution at interfaces. Considering the velocity range often found in seismic exploration, two or three different volume sizes (nh, $2nh$ and $4nh$ edges) at the layers can be used. Considering the possibility of local refinement at interfaces, more different sizes can be used to follow irregular interfaces and to guarantee a good G (points per wave length) at interfaces or at free surface using vacuum boundary condition, since it is known that a great number of points (about $G = 15$) is needed in interface (Robertsson, 1996). Further investigations will be made in next steps of the research to better investigate the numerical characteristics of the scheme, e.g., numerical dispersion, convergence and stability.

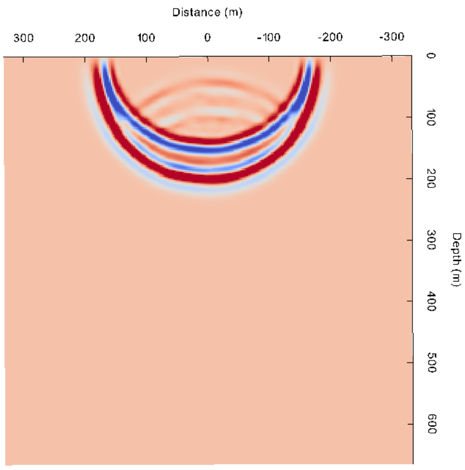

(a)

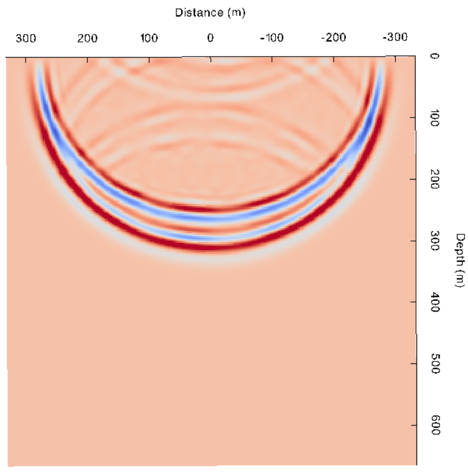

(b)

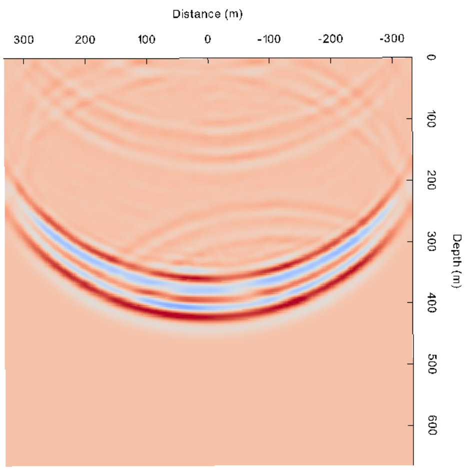

(c)

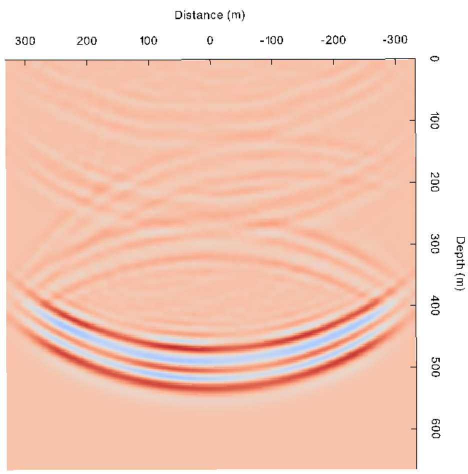

(d)

Figure 6: Snapshots at (a) $t = 0.224s$**, (b)** $t = 0.336s$**, (c)** $t = 0.448s$ **and (d)** $t = 0.56s$**.**

ACKNOWLEDGMENTS

The authors thank Jandyr Travassos, Eduardo Dutra, Franciane Peters, Cid Monteiro and Raphael de Souza by constructive conversations at LAMEMO / UFRJ.

REFERENCES

Bell, N., and M. Garland, 2012, Cusp: Generic parallel algorithms for sparse matrix and graph computations. (Version 0.3.0).

Berenger, J., 1994, A perfectly matched layer for the absorption of electromagnetic waves: Journal of computational physics, **114**, 185–200.

Cerjan, C., D. Kosloff, R. Kosloff, and M. Reshef, 1985, A nonreflecting boundary condition for discrete acoustic and elastic wave equations: Geophysics, **50**, 705–708.

Di Bartolo, L., C. Dors, and W. Mansur, 2011, A new finite difference scheme for modeling acoustic wave propagation: Presented at the 82nd Annual International Meeting, Society of Exploration Geopphysicists.

———, 2012, A new family of finite-difference schemes to solve the heterogeneous acoustic wave equation: Geophysics, **77**, T187–T199.

———, 2015, Teory of equivalent staggered-grid schemes: Application to rotated and standard grids in anisotropic media: Geophysical Prospecting, **to appears**.

Dormy, E., and A. Tarantola, 1995, Numerical simulation of elastic wave propagation using a finite volume method: Journal of Geophysical Research: Solid Earth (1978–2012), **100**, 2123–2133.

Graves, R., 1996, Simulating seismic wave propagation in 3d elastic media using staggered-grid finite differences: Bulletin of the Seismological Society of America, **86**, 1091.

Horesh, L., and E. Haber, 2011, A second order discretization of maxwell's equations in the quasi-static regime on octree grids: SIAM Journal on Scientific Computing, **33**, 2805–2822.

Levander, A. R., 1988, Fourth-order finite-difference P-SV seismograms: Geophysics, **53**, 1425–1436.

Moczo, P., J. Kristek, V. Vavrycuk, R. Archuleta, and L. Halada, 2002, 3D heterogeneous staggered-grid finite-difference modeling of seismic motion with volume harmonic and arithmetic averaging of elastic moduli and densities: Bulletin of the Seismological Society of America, **92**, 3042.

Reynolds, A. C., 1978, Boundary condictions for the numerical solution of wave propagation problems: Geophysics, **43**, 1099–1110.

Robertsson, J. O., 1996, A numerical free-surface condition for elastic/viscoelastic finite-difference modeling in the presence of topography: Geophysics, **61**, 1921–1934.

Virieux, J., 1986, P-SV wave propagation in heterogeneous media: Velocity-stress finite-difference method: Geophysics, **51**, 889–901.

Wapenaar, C. P. A., and A. J. Berkhout, 1989, Elastic wave field extrapolation: Redatuming of single- and multi-component seismic data: Elsevier Science Ltd, volume **2** *of* Advances in Exploration Geophysics.